AIAA 98-2878

Reynold Number Scaling at Transonic Speeds

M. L. Laster
Consultant
Tullahoma, Tennessee 37388

Egon Stanewsky
DLR
Goettingen, Germany

and

D. W. Sinclair and W. L. Sickles
Sverdrup Technology, Inc., AEDC Group
Arnold Engineering Development Center
Arnold Air Force Base, Tennessee 37389

19991202 067

20th Advanced Measurement and Ground Testing Technology Conference
June 15-18, 1998 / Albuquerque, NM

Reynolds Number Scaling at Transonic Speeds*

M. L. Laster**
Consultant
Tullahoma, TN

Egon Stanewsky
DLR
Goettingen, Germany

D. W. Sinclair and W. L. Sickles[†]
Sverdrup Technology, Inc., AEDC Group
Arnold Engineering Development Center
Arnold Air Force Base, TN 37389

Abstract

This paper focuses on Reynolds number scaling (RNS) at transonic speeds for military aircraft development. RNS has been used in the development of aircraft for decades because most development wind tunnels have not had the capability of providing full-scale flight Reynolds number. Any new, highly productive transonic wind tunnel that will provide duplicate flight Reynolds number up to 200 million (flight conditions of high-performance aircraft) is not likely to be built because of high cost. Thus, this paper discusses the importance of RNS and why it must be used for the foreseeable future. Two empirical methods and one computational fluid dynamics (CFD) method are shown to illustrate some of the issues and deficiencies involved with RNS. Wind tunnel effects on aerodynamic data that produce pseudo Reynolds number effects and that must be taken into account are also discussed. Finally, it is argued that improvements in RNS and proper accounting for wind tunnel effects on aerodynamic data can significantly contribute to the reduction in the time and cost of aircraft development.

Introduction

Why Reynolds Number Scaling (RNS)?

Interest in RNS comes from the fact that most conventional development wind tunnels are deficient in flight Reynolds number simulation by approximately an order of magnitude or more for nearly all aircraft aerodynamic configurations that have been or can be tested. This is true for the AEDC 16T, NASA 11 foot, NASA 12 foot, and many other commercial and foreign wind tunnels. High Reynolds number cryogenic wind tunnels such as the NASA National Transonic Facility (NTF) and European Transonic Windtunnel (ETW) approach flight Reynolds number simulation, but at a significant sacrifice in productivity. Thus, the need exists to be able to take low Reynolds number data from conventional production wind tunnels and predict flight performance, i.e. perform appropriate corrections to the data to account for Reynolds number mismatch. This is called Reynolds number scaling. Although not the primary subject of this paper, the need also exists to properly account for wind tunnel effects and measurement uncertainties on wind tunnel aerodynamic measurements. Both subjects are equally important for prediction of the flight performance of an aircraft design. Mack and McMasters discussed thoroughly the Reynolds number test needs for low-speed landing and takeoff situations for commercial transports.[1] This paper focuses on the Reynolds number issues in the transonic speed regime for military transports and high-performance aircraft.

Is RNS a New Issue?

RNS is not a new issue; its use in aircraft development has been an issue for decades. The problem is that the fidelity of RNS has always been poor, especially for transonic speeds where there is strong viscous/shock interaction. Today, RNS techniques are better termed an art than a science. Aerodynamic designers resort to a combination of empirical, semi-analytical predictions, and guesswork to accomplish a design. However, computational fluid dynamics (CFD) is increasing in utility and is being used more extensively in the design process, but it currently has many limitations, some of which will be discussed in this paper. Modeling of viscous flow phenomena for CFD is still imma-

---

** Associate Fellow, AIAA.

[†] Senior Member, AIAA.

Approved for public release; distribution unlimited.

American Institute of Aeronautics and Astronautics

ture for all but simple flows. Predictions of lift and loads are fairly well in hand. There are numerous turbulence models and a growing body of data. The weakness lies in CFDs ability to predict complex viscous flow phenomena such as separation, reattachment, unsteady effects that lead to buffet, transition from laminar to turbulent boundary layers, and strong shock boundary-layer interactions. Therefore, CFD is limited to design purposes and currently cannot be considered a reliable RNS tool. However, the need exists to assess its reliability for nearly all classes of military aircraft that fly in the low to transonic speed regime including large transports and high-performance aircraft. In time, perhaps the physics of these complex flows can be understood well enough that CFD can be a reliable design tool that computationally accounts for the right physics critical to simulation of off-design characteristics such as maximum lift and buffet onset. Later in this paper CFD calculations will be analyzed and discussed for a geometrically complex military aircraft configuration.

Comments on the Use of the Wind Tunnel

Deriving Aircraft Performance from Wind Tunnel Testing

To establish a basis for later discussion in this report, some of the fundamental principles for using wind tunnel data to predict flight performance are discussed in this section. The wind tunnel is not a perfect simulator of aerodynamic flight, and corrections to the wind tunnel data are needed if flight performance is to be accurately predicted. Today, the state of the art in correcting wind tunnel data does not accurately provide those needed flight predictions. Almost every military aircraft development has experienced significant surprises in aerodynamic performance and control in flight. The F-18E/F wing drop phenomenon is a recent example.[2] These surprises often result in costly retrofits, and even redesign. These events usually are very expensive, time consuming, and result in deployment delays, and/or degraded performance.

Current Philosophy in the Use of the Wind Tunnel

Until now, the philosophy regarding the use of the wind tunnel has been to optimize aerodynamic performance by testing different configurations, often just minor changes, and choosing the best. This philosophy has been successful in understanding performance differences of configurations and, therefore, there is confidence in this approach. The aircraft development community often tacitly assumes that tunnel effects are basically the same from one configuration to another, and thus, can be ignored while optimizing differences. This approach does not necessarily provide correct baseline configuration performance. Proper correction for tunnel effects and Reynolds number is needed to accurately predict flight performance.

The approach of optimizing configuration differences usually works better for new commercial aircraft development than for new military aircraft developments. This is true because new commercial aircraft configurations usually are evolutionary, incremental configuration changes from previous designs and have a large baseline of flight and wind tunnel data from which to base the new design. New military aircraft development programs usually do not have this extensive database because the new configuration is usually quite revolutionary from previous designs. Thus, new military aircraft are basically developed from "scratch," tailored with as much experience as possible. It is also true that new military aircraft of the same type are not developed as often as commercial aircraft.

The Wind Tunnel in the Aircraft Development Process

The wind tunnel is an integral part of the aircraft development process for design validation. Figure 1 schematically illustrates this. Development of a new military aircraft starts with concept definition,
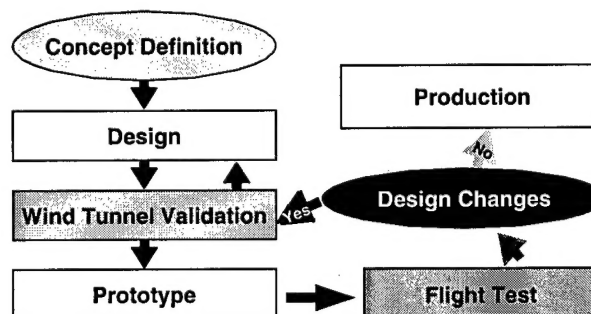

Fig. 1. Concept to Production (Development Testing Cycle.)

followed by its design. The aerodynamic conceptual design depends heavily upon analytical computations and, to some extent, upon wind tunnel data. Once design is begun, the aerodynamic lines need to be established early so that the structural and equipment packaging design can begin. Simultaneously, the aerodynamic design verification with wind tunnel testing is begun. The results of these tests feed back to the design, and the design is adjusted. These adjustments are usually checked with additional wind tunnel tests. After the design is frozen, a prototype is built, and flight tests are performed which often are not of the last configuration tested in the wind tunnel. Flight tests reveal how well the aircraft performs compared to design goals. If the design goals are met satisfactorily, a decision for production can be made. If the design goals are not satisfactorily met, redesign may be required if a degraded performance is not acceptable. Redesign usually brings on additional wind tunnel verification testing and additional flight tests. In the interest of acquisition reform, adequate RNS and test capability tools are important elements to achieve lower cost, reduced aircraft development time, and higher performance systems.

Thus, from concept definition to production, the wind tunnel is a critical part of the development process. It is used for experimental validation of the aerodynamic design of flight vehicles, including integration of the airframe and propulsion system. The goal of the design should be that the prototype flight vehicle works right the first time, design changes are not needed, and the performance is not compromised; i.e., the goal should be to eliminate the block called Design Changes in Fig. 1. Currently, this usually does not occur. Furthermore, the wind tunnel test community rarely knows how well they have done their job. Thus, a factual basis for improvements in the quality of wind tunnel data (information) for performance predictions and design is generally not available.

Proposed Philosophy in the Use of the Wind Tunnel

The ultimate objective in the use of the wind tunnel should be its contribution in the process required to accurately predict flight results within the bounds of acceptable uncertainty. This, argu-

ably, is an advanced philosophy and better use of the wind tunnel. But this use requires new and improved test technology so that correction for tunnel effects (flow quality, interference, aeroelastic) and Reynolds number can be accurately made. The rewards for this proposed approach can be huge. Closure on aircraft design should be faster and save on development cost. There should be fewer design iterations. There should be less flight testing because there is a better-designed prototype. The amount of wind tunnel testing should also decline with fewer design iterations.

Military Aircraft

Future Military Aircraft Requirements

Future high-performance aircraft, whether manned or unmanned, are expected to be low observable and highly maneuverable with long range and high payload capabilities. Carrier-operated aircraft will continue to need low-speed high-lift capabilities for take-off and landing. Configurations without tails are needed to satisfy the side low-observable requirement. High maneuverability most likely will require more than deflecting aerodynamic surfaces. Control jets are envisioned for this purpose. Long range and high payload mean high cruise lift/drag capabilities. Lateral stability and control can be a new, huge issue for these aircraft that are highly sensitive to Reynolds number effects. This adds even more emphasis to the need for improved and/or at least satisfactory RNS capabilities.

Future transport aircraft (both military and commercial) will need long range and high payload capabilities along with excellent low-speed, high-lift capabilities. Because existing conventional wind tunnels are expected to carry the preponderance of the development test load for the next several decades, all these needs will require added emphasis for a better capability to perform RNS. Specialty high Reynolds number wind tunnels such as the NASA NTF and the new ETW are expected to be used to validate RNS techniques, but they are unlikely to carry the high workload of development testing due to their lower productivity, intrinsic with their design for cryogenic operations.

Testing Criteria for RNS

Modern military aircraft fly in the range of 20 to 200 million Reynolds number at transonic speeds. A production transonic wind tunnel with this Reynolds number capability is not practical because of the high capital and operating costs. NASA and the Department of Defense jointly studied a new production transonic wind tunnel as a part of the proposed National Wind Tunnel Complex and found that capital cost would be in excess of one billion dollars to achieve a Reynolds number of 30 million.

Arguments have been made that the benefits of testing above about 10 million Reynolds number are quite small and that the residual Reynolds number effect is within the uncertainty of the data.[3] Reference 3 also argues and recommends that wind tunnel tests in the transonic speed range have a model RN, based on mean aerodynamic chord, between 3 and 9 million, but with swept wings, at least above 5 million. Reference 3 also states the tunnel turbulence level should be in the range of 0.5 to 0.75 percent for best extrapolation to flight. The testing of air ducts, control surfaces, etc. may be in a critical RN range where extrapolation to flight is not feasible; thus, full-scale testing is desirable in these cases. Reference 3 admits these criteria are not supported by conclusive evidence but are based largely on intuition tailored with experience. Today, 30 years later, there is evidence suggesting that many costly errors of flight performance prediction are attributed to inadequate RNS and Reynolds number test capability.

Current Practices in Reynolds Number Scaling

Large Aircraft

As mentioned previously, this paper focuses on the transonic cruise regime. However, let it suffice to say that RNS is a huge issue at low speed in the development of high-lift systems. Wind tunnel test capabilities in this regime are below flight RN values by factors of 2-6, depending on the size of the aircraft. Therefore, RNS is an issue at low speed as well. One can generally count on the boundary layer being turbulent over the majority of the aircraft in flight. However, this is not necessarily true for the wind tunnel model, where conventional tunnel Reynolds numbers are low. A majority of the

flow can be laminar under natural transition situations and be greatly influenced by the acoustical and turbulence level of the wind tunnel, which will tend to give the tunnel a slightly higher effective Reynolds number.

For large aircraft, range and payload performance are principal issues that translate into attention being focused on lift, drag, drag rise, and buffet boundary at transonic cruise conditions. Experience has shown that lift and pitching moment are usually not too sensitive to Reynolds number up to the onset of buffet; but, buffet boundary, maximum lift, drag, and drag rise are usually very sensitive to Reynolds number. Therefore, the aircraft developer is faced with accounting for Reynolds number effects with these parameters as best he can. The usual practice is to use a combination of test technique and empirical corrections. Because of little sensitivity of lift and pitching moment to Reynolds number below buffet onset, in most cases, the engineer has been able to directly use low Reynolds number wind tunnel measurements of lift and pitching moment in his design without having to resort to Reynolds number corrections. However, this is not necessarily true for wings with high aft loading. Test technique plays an important role in the determination of drag from wind tunnel data. Because the boundary layer is mostly turbulent in flight, experience has shown that forcing the model boundary layer to be turbulent in the wind tunnel makes the task easier in accounting for Reynolds number effects. Boundary-layer tripping is done on the whole model, but designers approach boundary-layer tripping in a variety of ways. Some position boundary-layer trips on the wing to match flight displacement thickness at the trailing edge. Some use a combination of forward and aft tripping to bracket the effect of wing shock position on drag. Once the wind tunnel drag measurements are available, the usual practice has been to adjust turbulent skin friction to flight Reynolds number. These techniques are not reliable whenever there are regions of separated flow on the aircraft. The prediction of and accounting for separated flow effects, which usually is a strong function of Reynolds number, is still an area needing much research to understand the physics and analytically model its behavior. In general, the philosophy of large aircraft design has been to prevent or

avoid separated flow at normal cruise conditions. The prediction of buffet boundary and maximum lift is still an experimental and empirical art for the most part. Some attempts are being made with Navier Stokes (NS) CFD techniques to predict these parameters. In a recent survey of industry practices by the authors, results reveal that CFD is being used in a complementary role to wind tunnel testing. NS calculations of lift, not buffet boundary and maximum lift, do a reasonable job; but absolute drag calculations have proven inadequate and not reliable. However, CFD improvements are expected and will aid the designer once validated codes are developed. CFD, as compared to the wind tunnel, also grossly suffers from a lack of productivity. A single data point for NS CFD requires days, sometimes weeks, to compute, compared to the wind tunnels, which can produce on the order of 100 data points per hour.

High-Performance Aircraft

RNS as applied to high-performance aircraft in cruise has been mainly devoted to drag corrections. Interest here lies in the fact that these aircraft are designed for range, payload, and loiter time over targets. Other than drag, there has not been as much concern for RNS with other aerodynamic parameters. Most designers claim, via experience, that high-performance configurations with thin wings and large tails are not subject to significant RN effects. The techniques used to scale drag to flight are somewhat similar to large aircraft techniques. There is little concern with buffet for example. Such aircraft are designed to power their way through maneuver conditions. However, future high-performance aircraft, especially those that have no tails for low observable purposes, most likely may be sensitive to severe RN effects in lateral stability. There is some experimental evidence which highlights this concern (see Fig. 2). Note especially the rolling and yawing moment. To the authors' knowledge, little work has been done to understand the extent of this problem. Therefore, techniques to deal with RNS need development.

Pseudo Reynolds Number Effects and Test Technique

There are a number of wind tunnel and model effects which affect model aerodynamics in a man-

ner that can be misinterpreted as Reynolds number effects. Care must be taken in wind tunnel testing to ensure that these pseudo RN effects are taken into account, especially if a test objective is to evaluate actual RN effects on aerodynamic data. These pseudo RN effects are generally well known and have been discussed at length in various papers and reports. Reference 4 treats this subject extensively. Pseudo RN effects have been observed related to tunnel calibration, wall interference, flow quality, temperature nonequilibrium, surface roughness, and model deformation. Often, it is very difficult to separate all the parameters which produce pseudo RN effects. However, as much care as possible must be taken to assess RN effects accurately.

In attempting to study RNS and using data from more than one wind tunnel or source, test technique is important to minimize the number of test variables that otherwise can make it impossible to evaluate Reynolds number effects. Haines[5] adds to this by emphasizing the necessity of "knowing your flow."

Reynolds Number Scaling and Viscous Simulation

All who perform RNS use some methodology. However, many methodologies are proprietary in industry, which is one reason why AGARD Working Group 09 developed a methodology[6] for common use. It suggests that the synergistic use of CFD calculations and wind tunnel testing would alleviate some of the limitations for estimating aircraft performance inherent in both of these methods.
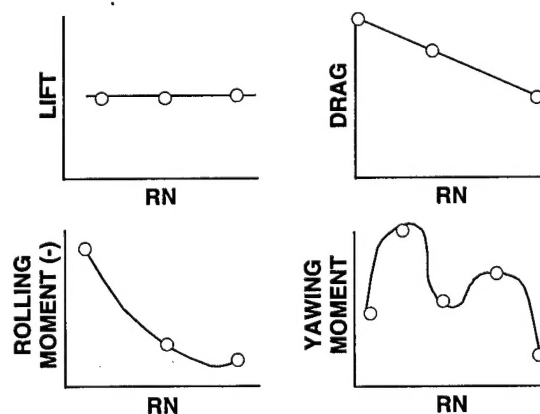

Fig. 2. Example of RN effects on a low observable aircraft.

AGARD Viscous Simulation Methodology

The AGARD Methodology's primary focus is concerned with the duplication of the flow development that occurs at the high Reynolds numbers of flight in low Reynolds number wind tunnel tests by following certain rules of boundary-layer manipulation. The methodology is far more than deciding how and where to fix transition, and requires actions before, during, and after the wind tunnel tests. The basic elements of the AGARD methodology are:

1. Collect information on the wind tunnel, the vehicle to be tested, and objectives of the test program.

2. Predict differences between model and flight scales.

3. Perform wind tunnel tests.

    a. Obtain data for free transition and forward tripping.

    b. Determine viscous effects by boundary-layer manipulation.

3. Extrapolate the results to flight conditions.

The methodology is dependent on the wind tunnel being used and how the flow in the tunnel affects the configuration being tested. Some apparent (pseudo) Reynolds number effects can arise from variations of empty tunnel flow calibration, turbulence, acoustic noise, and wall interference with unit Reynolds number of the flow. The prediction of differences between model and flight scales requires that the pseudo-Reynolds number effects be identified and eliminated from the test data. Therefore, it is imperative to have detailed information about the facility flow, and to be able to estimate the effects of the facility flow on the particular configuration to be tested.

To apply the methodology, data trends must be predicted before the test so that the proper test conditions and trip locations can be selected. The most advanced computational methods available should be used to calculate data trends from the model-scale through flight-scale Reynolds num-bers. As a minimum requirement, the computations should be made for a three-dimensional wing-body configuration with a code that is capable of calculating weak viscous-inviscid interactions. Ideally, a computational technique that accurately accounts for strong viscous-inviscid interactions such as flow separation is desirable, but currently unavailable.

The initial wind tunnel tests involve free transition and transition fixed at the forward location where transition is expected at flight scales. The objective of the initial tests is to determine the sensitivity of the results to changes in the boundary layer. If the difference between the tripped and free transition data is insignificant, then nothing will be gained by tripping at more rearward locations.

Prediction of Boundary-Layer Transition

For accurate calculation of the forces (especially drag), the location of transition of the model boundary layer from laminar to turbulent must be accurately predicted, measured, or fixed. Otherwise, in the case of transonic flow, the shock/boundary-layer interaction cannot be properly modeled. For transition fixing, the prediction of the untripped transition location is important to assure that the boundary-layer trips are placed ahead of the location where transition occurs "naturally" in the test facility. The transition location is dependent on the pressure gradient, surface roughness, turbulence and/or noise, and instabilities associated with the three-dimensionality of the flow. Therefore, the location of transition is both model- and flow-field dependent.

A transition prediction technique should account for the model geometry and the effect that tunnel flow quality has on the stability of the boundary layer. At low angles of attack and for moderately swept wings, a simple approach described in Ref. 7 has given good results at the mid-span, where the flow is essentially two-dimensional. As expected, the agreement becomes worse as three-dimensional effects begin to dominate, such as at the wingtip and wing/body juncture. The method described uses a three-dimensional, full-potential code coupled with a two-dimensional boundary-layer code to calculate the growth of the laminar boundary layer for the particular model geometry.

Existing empirical data from 23 wind tunnels throughout the United States and Europe,[8-9] as well as flight[9-10] for an ultra-smooth, 10-deg cone, were used to provide transition criteria for each test facility where data were available.

In the original study, data from all the wind tunnels were correlated with measurements of cone surface pressure fluctuations. It is recommended that data from the facility where the test is to be performed be used to estimate transition location rather than applying the correlation based on all the tunnels. This recommendation is based on the observation that the individual tunnels do not necessarily follow the trend derived from all of the data. Porous wall transonic wind tunnels, which have high levels of edge-tone noise generated by the numerous holes in the walls, were found to have transition Reynolds numbers that were lower than those measured in flight. This result seemed to be consistent with observations made at supersonic Mach numbers, which showed transition Reynolds number to be inversely related to noise. However, in some cases, the transition Reynolds number was independent of noise level, and in other cases, the transition Reynolds number actually increased with increases in noise level. This observation suggested that transition on the cone was affected by factors in addition to the noise level.

Measurements made in the AEDC Tunnel 16T after the installation of screens and honeycomb in the stilling chamber were compared with measurements from Ref. 8 and reported in Ref. 11. The installation of the screen and honeycomb in the tunnel did not significantly alter the noise measured on the cone surface; however, measurements of total pressure fluctuations were approximately $1/6^{th}$ of the values prior to the installation of the screen and honeycomb. At subsonic conditions, there was an increase in transition Reynolds number of approximately 20 percent, even though the noise measured on the cone surface did not change. The new values of transition Reynolds number shown in Ref. 11 are comparable to flight values at similar unit Reynolds numbers. At supersonic Mach numbers, the improvement in transition Reynolds number decreased with increasing Mach number until no improvement was seen at a Mach number of 1.6. These results confirm that the measurement of the magnitude of broadband noise does not correlate well with transition location. The spectrum of the noise is probably more important. Stability analysis of boundary layers shows that disturbances in the boundary layer are selectively amplified or damped, and that the magnitude of the disturbances must grow to a critical value before transition to turbulence occurs.

The instrumentation commonly used to measure noise and turbulence (i.e., microphones and hot wires) is sensitive to both pressure and velocity fluctuations, and the effect from each parameter is difficult, if not impossible, to separate. In a solid wall tunnel, the spectrum from both instruments is free of discrete frequencies that can significantly affect the integrated overall level. This means that an increase in the overall level will be the result of a proportionate increase at each frequency. Therefore, in a solid wall tunnel, one would expect a correlation between noise or turbulence measurements and transition. In a porous wall wind tunnel, the spectra from microphones and hot wires will typically contain discrete tones that are characteristic of the holes in the walls. The absence of discrete tones is an indication that the background turbulence level is greater than the noise generated by the wall porosity. The presence of the discrete tones can alter the overall noise level as different resonance conditions of the wall and surrounding plenum chamber are encountered. The overall level is no longer uniquely correlated with the magnitude at each frequency in the spectrum; therefore, the overall level may not result in a proportionate change at the frequencies that are amplified by the boundary layer, and transition will not be correlated to overall noise level. A better way of correlating noise and transition may be to integrate the noise only in the frequency range that is amplified by the boundary layer. This approach would require a boundary-layer stability analysis to determine the critical frequency range as a function of the laminar boundary layer on the model and the flow conditions.

An Example of Reynolds Number Scaling

The prediction of full-scale results should involve both experimental and computational

results. In general, the measured trends should be extrapolated to an effective Reynolds number where strong viscous-inviscid interaction present at the model scale disappears as Reynolds number is increased. The calculated trend should be used to extrapolate from the critical Reynolds number to the flight condition.

Experimental Database

In the following sections, the empirical and computational RNS approaches are evaluated using the experimental database acquired under a cooperative effort between the United States Air Force and the German Ministry of Education and Science, Research and Technology (TST program). The TST database is a unique, comprehensive set of low-speed and transonic data that were obtained from five wind tunnels, which include AEDC Tunnel 16T and the National Transonic Facility (NTF). Data were obtained over a broad range of Reynolds numbers from low Reynolds numbers obtained in conventional wind tunnels (i.e., 16T) to matching flight Reynolds numbers obtained in the high Reynolds number wind tunnels (i.e., the NTF). The objective of the test program was to develop a quality database for studying the interaction of tunnel-environment, wall-interference, and Reynolds-number effects that prevent wind tunnel data from being totally representative of flight.

The experimental data represent eight tunnel entries, including four from the 16T and NTF. The decision was made early on to use one model and sting in all tests performed and use the same personnel to assemble the model in each test. The number of balances was mini-

mized, but redundant data were taken whenever more than one balance was used to ensure identical measurements. Multiple balance calibrations were employed. Wall pressures were measured to evaluate wall interference when practical. Boundary layer tripping was employed at identical conditions and locations from one wind tunnel to the other. In non-tripping tests, boundary-layer transition location was measured when possible. Test conditions were overlapped in Mach number and RN from one tunnel to the other to provide a base for evaluating differences in tunnel effects and determining their cause.

The test article used for the effort was a 1/10-scale model of the Dornier Alpha Jet Technology Demonstrator with the TransSonischer Tragflügel (TST wing), a transonic technology wing. The test article was built to cryogenic testing standards and had a surface finish of 0.2 μm (7.87 x 10^{-6} in.). The dimensions of the test article are shown in Fig. 3, and a schematic of the instrumentation is shown in Fig. 4. The database contains a comprehensive set of measurements including both conventional (balance and pressure taps) and nonconventional measurements. Pressure taps were located on the
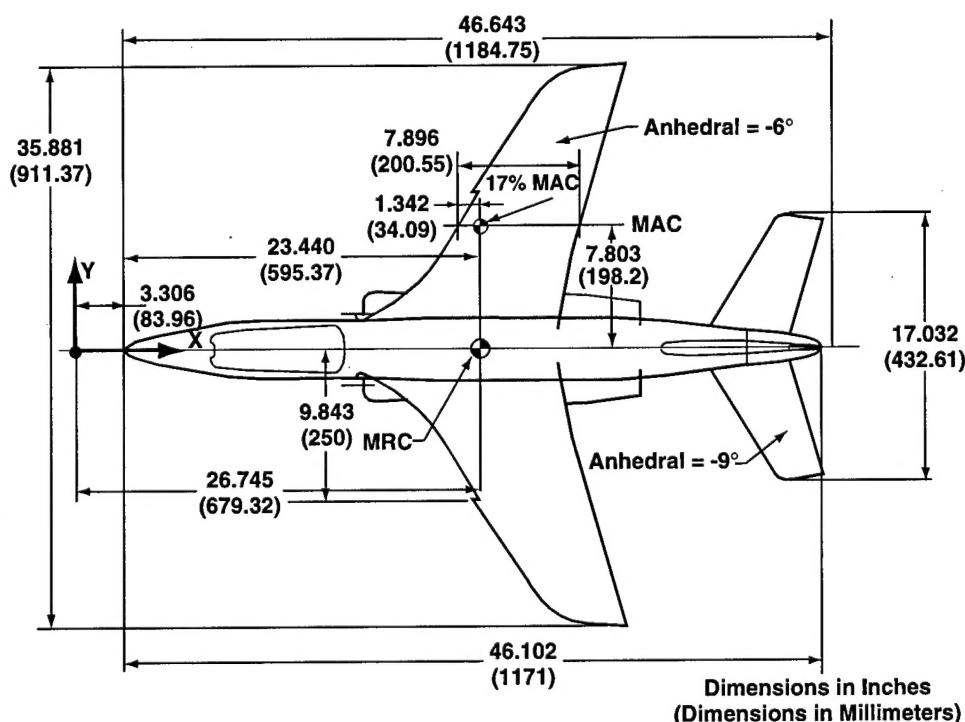

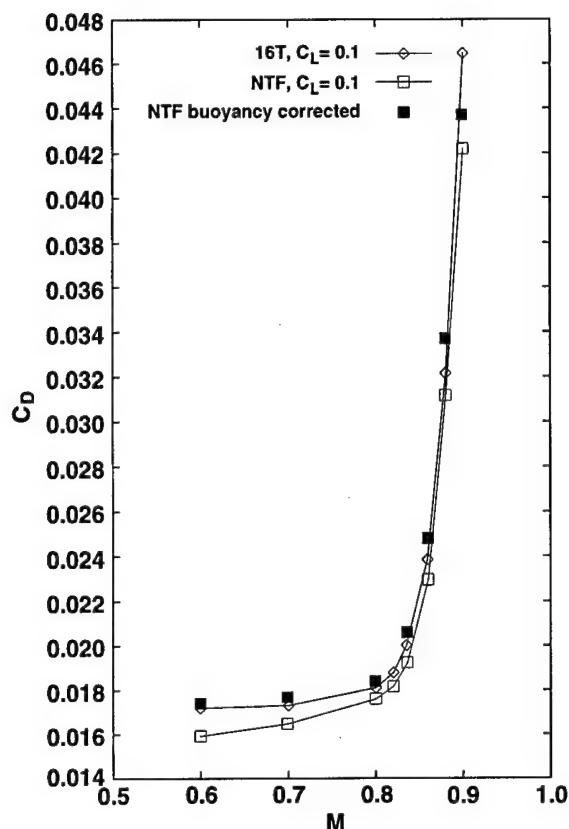Fig. 3. TST model dimensions, top view.

Additionally 2 Balance Cavity Pressures and 1 Sting Thermocouple TB, 1, R

Balance NTF 105/3 Thermocouples TS, 1, P

Heated ESP Box
- 4 48SL PSI Scanners
- 2 Temperature Resistors PT, 1-2, M
- 1 Thermocouple TC, 2

Thermocuple Balance Adapter TB, 1, F

1 Dynamic Pressure Sensor KN, 1

7 Steady-State Pressure Tappings on Canopy PC, 1-7

Thermocouple Innerside Bow TL, 1

Heater Inclinometer Box
- Q-Flex Inclinometer I, 1: T, 1
- 2 Accelerometers A, I, Z/Y
- 4 Spectron® Bubbles B, 1-B, 4
- 2 Temperature Resistors PT, 1-2, 1
- 1 Thermocouple TC, 1

Y Dimensions in Millimeters

Thermocouple at Strain Gage TW, 1, P

Thermocouple TW, 2, P

Thermocouple TW, 3, P

Thermocouple TW, 4, P

Accelerometer TW, 1, P

Thermocouple TW, 1, S

Accelerometer AW, 1, S

169 Steady-State Pressure Tappings in 5 Sectins PW (I-V), 1-34-S

Balance

Thermocouple TS, 1, P

Strain-Gage Root Bending SG, 1, P

3 Steady-State Pressure Tappings Inside Nozzle PN, 1-3, P

5 Dynamic Pressure Sensors 40, 50, 60 ,70, 75% c_local Kw, 5-1, P

Y 400, Y 295, Y 200, Y 100, Y 65, Y 200

Fig. 4. Overview of model instrumentation.

canopy, on the upper and lower wing surfaces at five spanwise locations, in the duct exit, and in the balance cavity. Additional pressure taps were added to the aft fuselage after the initial 16T and NTF tests and prior to the final 16T test. The non-conventional measurements included pressure sensitive paint (PSP), infrared transition detection, liquid crystal, and multi-element film. In addition to these measurements, wing-wake and duct-exit total pressures were obtained by removing the tail and installing a rake apparatus. The wing-wake measurements are of value in evaluating the accuracy of the turbulence models, which will be seen later. Data also exist for a variety of boundary-layer trip configurations.

Corrections for Tunnel Effects

The TST model is extremely small in 16T (0.14 percent blockage ratio), while the model is a typical size for NTF (0.44 percent solid blockage ratio). Because of the low blockage ratio in 16T, the data are assumed to be free of wall interference. Figure 5 shows a comparison of the drag coefficient vs.

Mach number (drag rise) between 16T and NTF at matching conditions. The drag coefficients in NTF are lower than 16T. A buoyancy correction is estimated by determining the difference between the 16T and NTF forward and aft fuselage pressures and assuming a linear distribution over the model for the pressure difference. This buoyancy correction would include both the clear tunnel and model-induced effects. However, corrections for clear tunnel buoyancy from the tunnel-empty calibration were determined to be less than a drag count; therefore, this correction will be a model-induced or wall interference effect. Correcting the NTF data for this assumed buoyancy dramatically improves the tunnel-to-tunnel agreement between 16T and NTF (see Fig. 5). Therefore, it is assumed that the difference in drag between the tunnels is dominated by wall interference. Since the lift and pitching-moment coefficients agree reasonably well, it appears that the wall interference manifests itself predominantly as a buoyancy effect. The data presented in the remainder of this report are not corrected for buoyancy effects.

Fig. 5. Comparison of drag coefficient versus Mach number for Tunnels 16T and NTF, $R_{EC} = 3.3 \times 10^6$, no trips.

Corrections for the effects of free-stream turbulence or vorticity have not yet been attempted for any of the data obtained in these experiments. However, it is reasonably well understood that free-stream vorticity tends to increase turbulent skin friction drag. For any aircraft development program, the magnitude of the wind tunnel vorticity effect (as well as other flow quality effects) on drag should be known. This means that the vorticity or turbulence level of each wind tunnel used should be known, and research should be carried out to quantify its effect on drag.

Empirical RNS of Drag

Two empirical techniques are employed to estimate drag at flight Reynolds numbers using low Reynolds number wind tunnel data: (1) turbulent skin friction corrections and (2) least-squares extrapolation.

In the case of drag, the procedure of simply correcting for the effect of Reynolds number on skin friction can give less than satisfactory results. In Fig. 6, the total drag measured in Tunnels 16T and NTF for a Mach number, M, of 0.6 at an angle of attack, α, of 2.0 deg (C_L approximately equal to cruise) is presented as a function of Reynolds number. When the boundary layer on the model is allowed to transition naturally (i.e., no trips), there is very little change in drag below a Reynolds number of 10×10^6, and decreases at Reynolds numbers greater than 10×10^6. Simple extrapolation of the low Reynolds number data for the untripped model would not predict the decrease in drag. Without tripping, the drag measured in the NTF is approximately 10 drag counts lower than Tunnel 16T at matching Reynolds numbers of 2.7 and 3.3×10^6. The difference in drag is still present when the boundary layer is tripped on the wing only, and in some cases, the difference increases when trips are used. It is believed that this drag difference is a model-induced buoyancy effect. The agreement between the turbulent flat plate drag estimated for the model and the fully tripped data from Tunnel 16T is excellent. Also, the agreement with the untripped data for the NTF at the higher Reynolds numbers is very good; however, this result may be fortuitous, since a correction for the lower drag at the lower, matching Reynolds number has not been made. When the skin friction trend is corrected to the NTF data measured at a Reynolds number of 10×10^6, the trend underestimates the drag at 20×10^6. This is also true at other angles of attack.
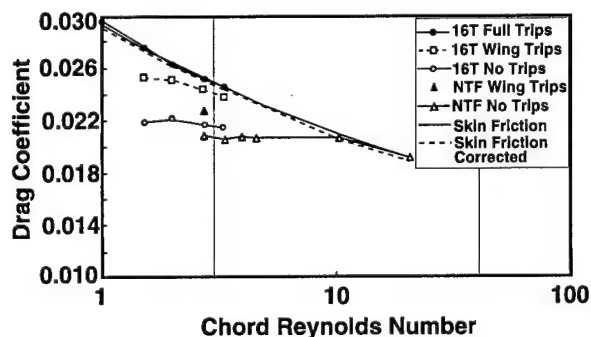

Fig. 6. Drag as a function of Reynolds number for M = 0.6, α = 2.0 deg.

In Fig. 7, the total drag measured in the same wind tunnels for a Mach number of 0.835 and angle of attack of −1.0 deg for the same model is presented. The same general differences between the tunnels observed at a Mach number of 0.6 are present at these conditions. The estimated turbulent flat plate drag trend does not follow the trend of the fully tripped data from Tunnel 16T or the trend of the untripped model at the higher Reynolds numbers. This was also true at higher angles of attack.
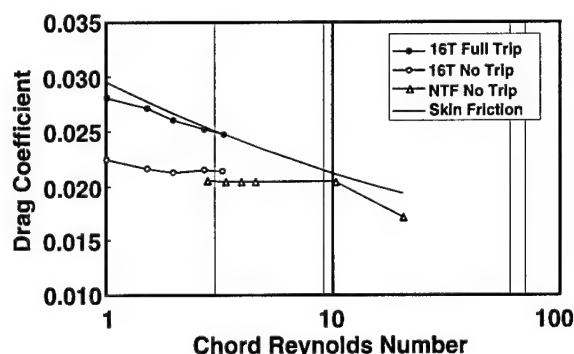

Fig. 7. Drag as a function of Reynolds number for M = 0.835, α = -1 deg, skin friction trend.

In Figs. 8, 9, and 10, a trend derived by a least-squares fit of a power function of the form:

$$C_D = A \times Re^B$$

using the fully tripped data from Tunnel 16T was used to predict results at higher Reynolds numbers for a Mach number of 0.835. The trend was corrected to the NTF drag measured at a Reynolds number of 10×10^6. The corrected trend overestimates the values at the higher Reynolds numbers.
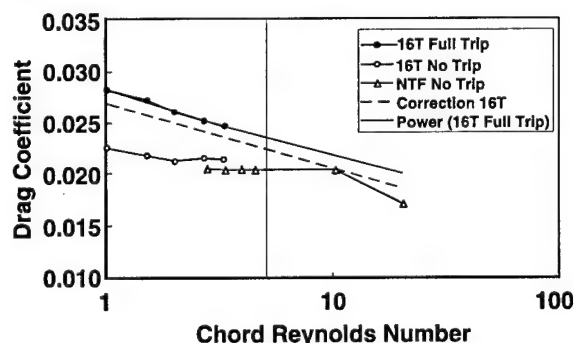
Fig. 8. Drag as a function of Reynolds number for M = 0.835, α = -1 deg, full trip trend.
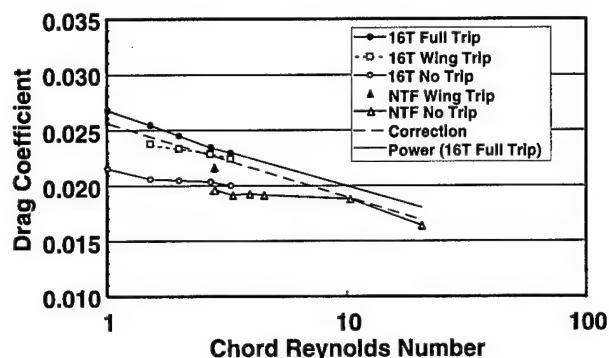
Fig. 9. Drag as a function of Reynolds number for M = 0.835, α = 0 deg, full trip trend.
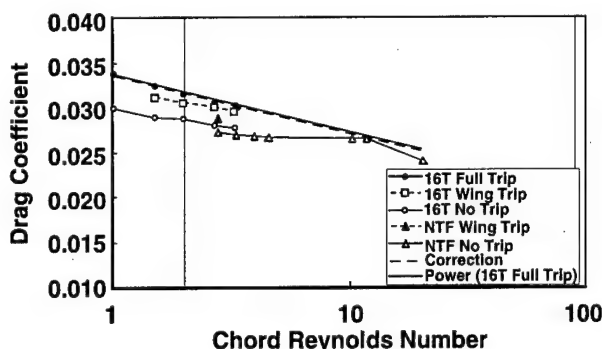
Fig. 10. Drag as a function of Reynolds number for M = 0.835, α = 2 deg, full trip trend.

The conclusion that can be reached is that a simple empirical correlation using either flat plate skin friction drag or fully tripped Reynolds number trends can give inconsistent results. The underlying assumption with these techniques is that the significant features of the flow field such as separation are present or absent at all Reynolds numbers (i.e., no major changes in the character of the flow). It is rare that this is true over a wide range of Reynolds numbers; therefore, the extrapolation process requires the prediction of a trend that accounts for the physics of the flow. This suggests the need for CFD.

Computational Investigation

The objective of the computational investigation is to evaluate the current CFD capability as a Reynolds Number Scaling (RNS) technique for transonic flow conditions. The approach is to use the latest codes and turbulence models to perform the computations about the TST configuration and to use the test data to evaluate the results.

Computational Approach

The chimera overset grid approach[12-13] was used for the CFD calculations. The approach is a domain decomposition technique which allows a complex configuration to be divided into manageable components or regions. A grid can then be generated for each component or region. This facilitates grid generation and allows the modeling of very complex shapes. The chimera approach also provides for communication among the overlapped grids. To improve interpolation accuracy among the grids, the current computations utilize double-fringe interpolation stencils.

The flow solver employed to obtain three-dimensional steady-state flow-field solutions was the chimera implementation of a finite-difference algorithm developed by Tramel and Nichols.[14] The algorithm is an upwind flux formulation combined with a quasi-Newton relaxation time-stepping strategy.

The computations were performed for fully turbulent flow using the K-ε two-equation turbulence model of Nichols[15] which is based on the model of Speziale, et al.[16] To reduce the number of points required to model the boundary layer accurately, the near-wall region was approximated using the wall function implementation of Nichols.[17] The wall function is based on the law-of-the-wall of White and Christoph.[18] Turbulence modeling and appropriate calibration of the models for variations in free-stream turbulence or vorticity continue to be the major impediment in obtaining accurate computational simulations or, more specifically, in obtaining accurate prediction of drag and separation. However, the two-equation models, such as K-ε and K-ω models, represent the state of the art and are widely used in the CFD community.

The TST model grid system shown in Fig. 11 consists of 27 individual meshes and a total of approximately six million points. Every detail of the model is represented, including the flow-through inlet, the inlet diverter and inlet gutter, the sting, the notch in the wing leading edge, and the thickness of the wing trailing edge. The wing meshes are c-meshes with constant spanwise sections at the array locations of the wing pressure orifices. To capture the wake flow, an h-mesh is included downstream of the wing. The horizontal tail mesh is an o-mesh topology. Wherever possible, direct injection was used to get the best possible mesh-to-mesh communication. The far-field boundary was positioned approximately ten body lengths away. The first point off the surface of the model was positioned to give a y+ of approximately 25 at a chord Reynolds number, Re_c, of 2.7×10^6.
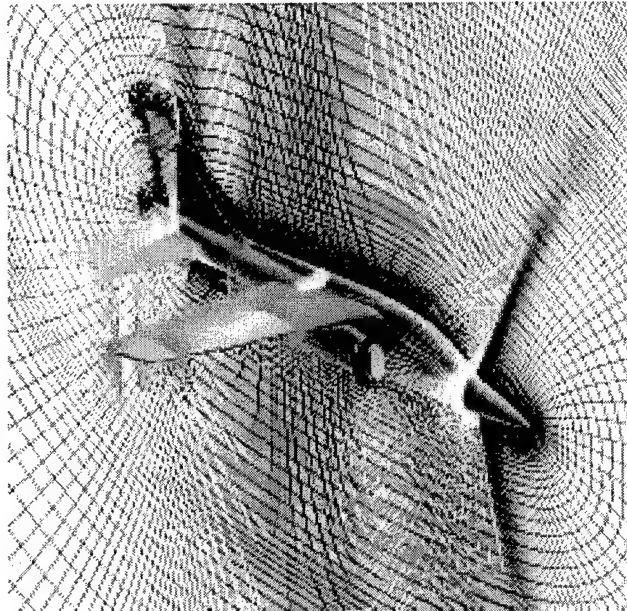

Fig. 11. TST grid system.

Computational Results

Convergence of the steady-state computational results about the TST configuration was monitored by computing the forces and moments using FOMOCO.[19] When the computed load coefficients did not change between successive runs to four decimal places, the solution was declared converged.

Table 1 shows the flow conditions for which computational results were obtained. The computations were performed for several angles of attack

Table 1. TST Transonic Navier–Stokes Computations

Mach No., M	α, deg	Reynolds No. ($Re_c \times 10^6$)	Turbulence Model
0.835	0	2.7	K-ε
0.835	2	1,2.7,10,20	K-ε
0.835	4	2.7	K-ε

at the transonic Mach number of 0.835 (cruise Mach number). To predict Reynolds number trends, several Reynolds number solutions were performed at 2-degrees angle of attack (approximate cruise angle). The Reynolds number range covered the entire range of tested Reynolds numbers, which included matching low Reynolds numbers obtained in 16T and flight Reynolds numbers obtained in the NTF.

Whenever possible, the predicted results are compared to wind tunnel measurements such as wing, canopy, and rake pressures as well as balance measurements. The computations are compared to wind tunnel data obtained with trips positioned near the nose of the fuselage, on the interior and exterior of the forward inlet, at approximately the 10-percent chord position of the wing and the tails. In addition, the predicted pressures are also compared to PSP measurements. The PSP results were obtained without trips, although the paint does promote an earlier transition of the flow.[20]

Representative comparisons between predicted and measured pressure are shown in Figs. 12-13 for $\alpha = 2$ deg and $Re_c = 2.7 \times 10^6$. Figure 12 shows the comparison between the computed model pressure distribution and the PSP measurements. Qualitatively, this comparison looks very good, even though boundary-layer transition in the computations is probably forward of the transition loca-
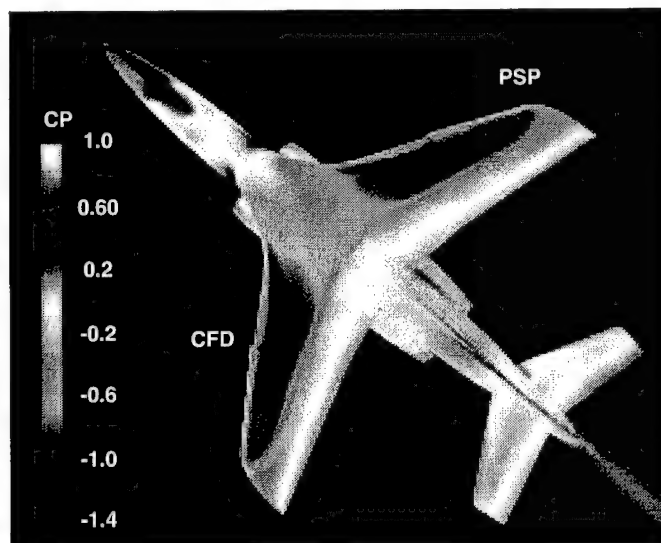

Fig. 12. PSP and CFD pressure coefficients comparison, M = 0.835, $\alpha = 2$ deg, $Re_c = 2.7 \times 10^6$.

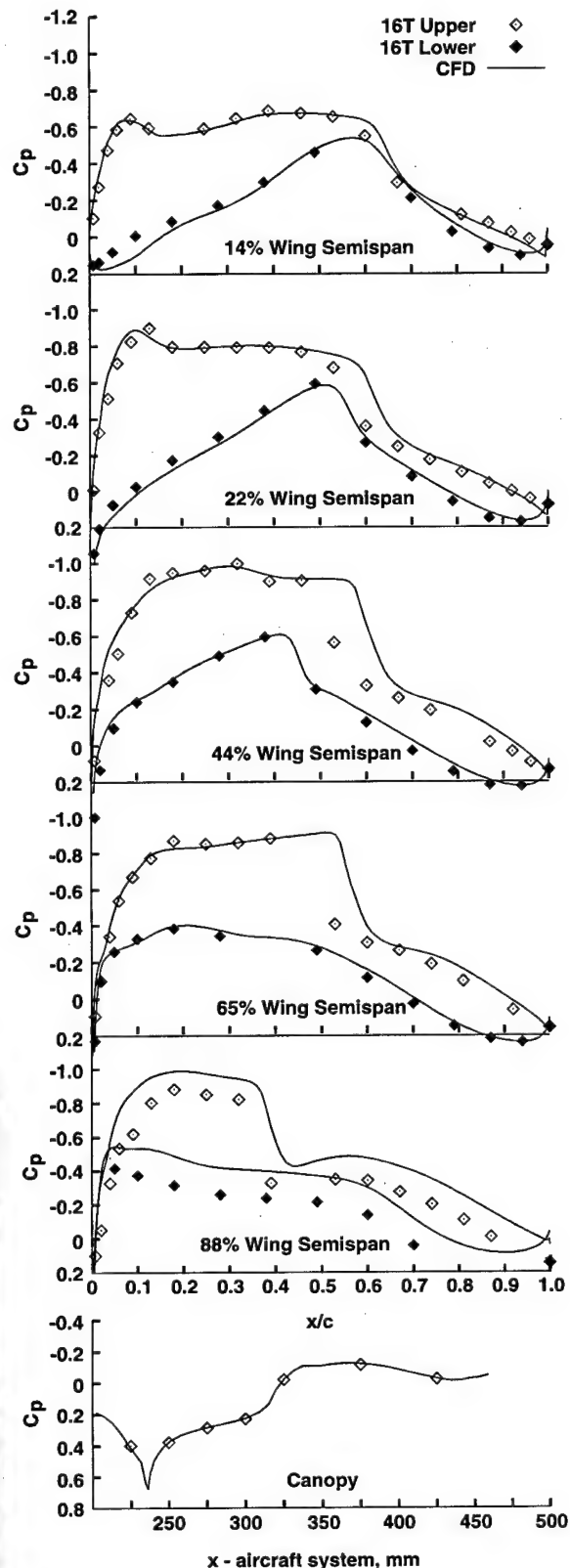
Fig. 13. Measured and computed model pressures, M = 0.835, $\alpha = 2$ deg, $Re_c = 2.7 \times 10^6$, full trips.

tion with PSP. The spillage around the inlet appears to be computed accurately, as well as the wing shock structure.

Figure 13 shows the comparison between the predicted pressure distribution and the pressure orifice measurements for both the wing and the canopy. The excellent agreement on the canopy indicates the free-stream Mach number in both the tunnel and in the computations is the same. The predicted pressure on the lower wing surface shows excellent agreement with the data. However, the predicted upper surface distribution shows a shock that is slightly stronger and positioned downstream of the measurements.

Figure 14 shows the computed model pressure distribution with varying Re_c. Here the expected trend is seen, i.e., the shock moves aft and steepens with increasing Re_c. Similar results at $\alpha = 0$ deg and $Re_c = 2.7 \times 10^6$ were obtained. In general, there is agreement, but as will be seen, small differences in pressure distributions can yield noticeable differences in integrated loads.

Figure 15 shows the comparison between the predicted and measured wing-wake total pressure. The difference between the computations and the data is much larger than the effects of tripping the boundary layer based on uncorrected high Reynolds number data. The computations are showing a larger pressure deficit than the measurements. This deficit indicates that the turbulence model is overpredicting the momentum losses and skin friction. This predicted momentum loss is caused by the turbulence model and originates either from the outer-layer K-ε model or the sub-layer wall-function model. The result from the larger skin friction and the aforementioned pressure differences is that the prediction of the computed drag is much higher than the measurements, which is clearly seen in the comparison of the computed and measured loads in Fig. 16. The computed drag coefficient is approximately 25 counts (0.0025) higher than the measured drag coefficient. The comparison of lift and pitching moment is much better. Other investigators have had similar experiences in attempting to predict drag with CFD, especially on aircraft equipped with supercritical wing shapes such as the Onera-M6 wing.[21]
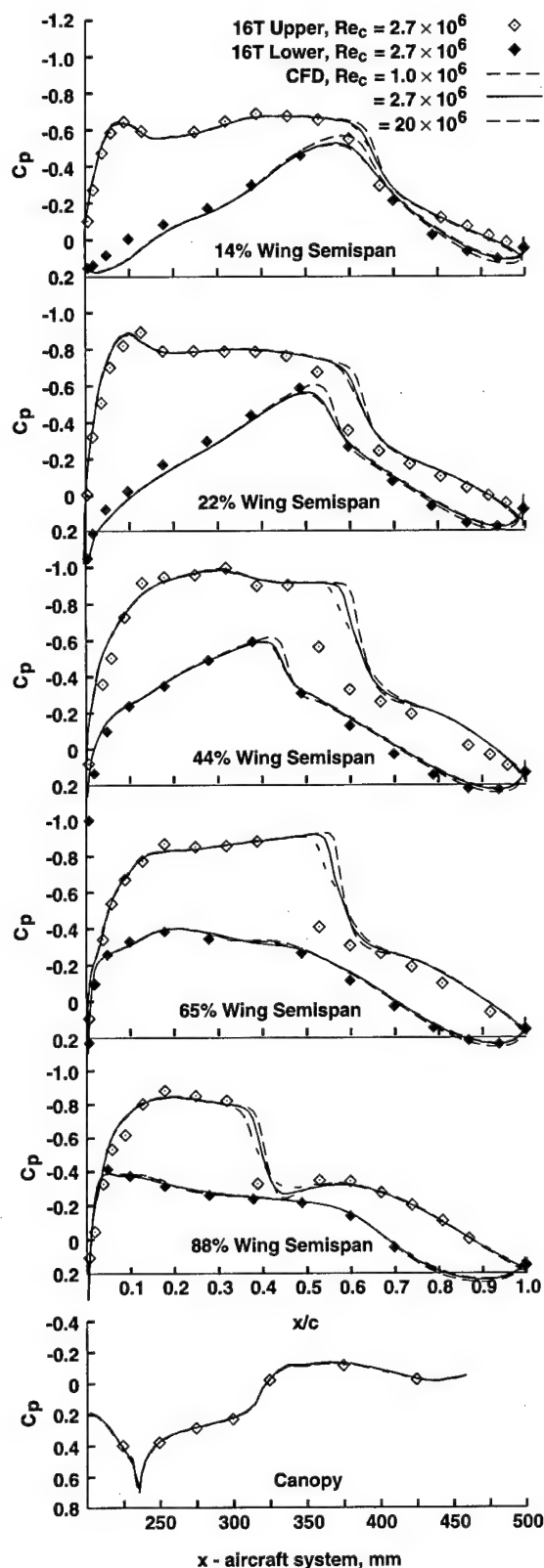

Fig. 14. Measured and computed model pressures, M = 0.835, α = 2 deg, various Re_c, full trips.
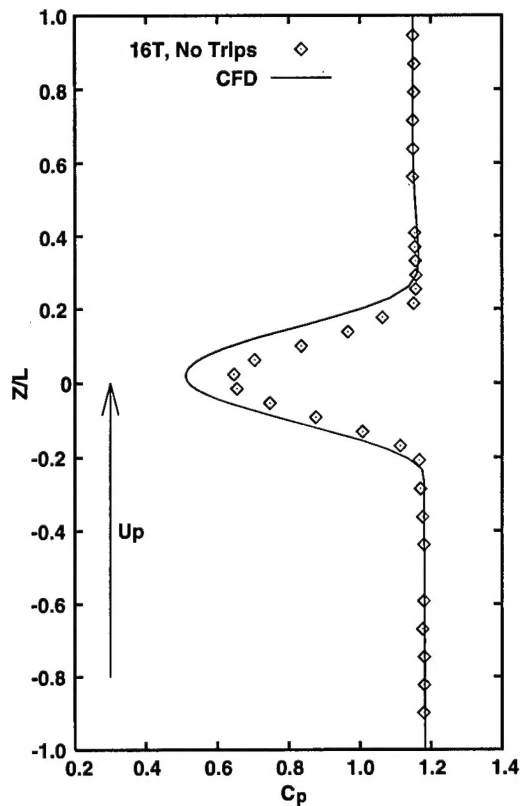
Fig. 15. Measured and computed wake pressures, $M = 0.835$, $\alpha = 2$ deg, $Re_c = 2.7 \times 10^6$.

The comparison between the measured and computed duct-exit rake pressures is shown is Fig. 17. The computations show a slightly higher total pressure loss in the center of the duct while reasonable agreement is shown in the boundary layer. Although the duct flow was not tripped in the experiment, analysis indicates that transition occurs early in the duct; therefore, the experimental duct flow should be predominantly turbulent. The difference in the duct flow contributes to the drag difference between the data and computations by altering the duct and spillage drag. Estimates of the duct drag and spillage were determined from the experimental and computed rake pressures. The computations predict a duct drag that is approximately one drag count higher and a spillage that is approximately 3 percent higher. The contribution to the external drag due to difference in spillage was not determined. Although a factor, the difference in duct flow does not appear to be the major contributor to the drag difference between the computations and data. The major contributor appears to be a higher external drag caused by the higher
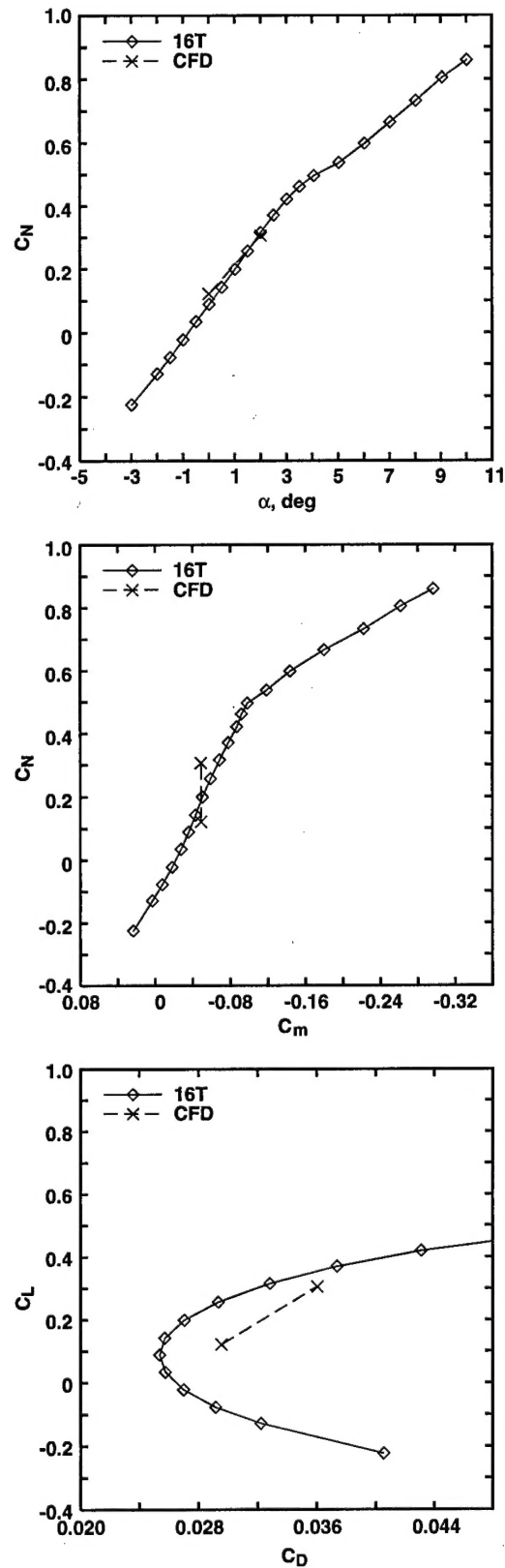

Fig. 16. Measured and computed forces and moments, $M = 0.835$, $Re_c = 2.7 \times 10^6$, full trips.
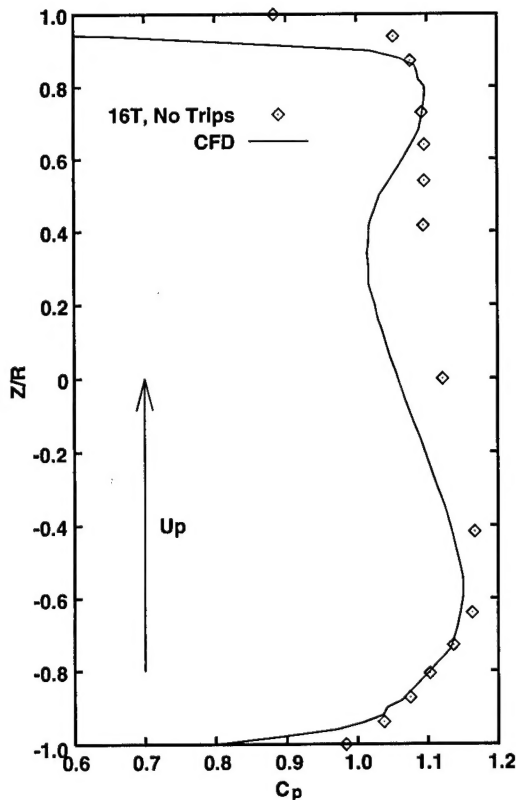
Fig. 17. Measured and computed duct-exit pressures, M = 0.835, α = 2 deg, Re_c = 2.7 $\times 10^6$.

external skin friction drag predicted by the turbulence model. Improvement in the absolute prediction of drag could be gained by tuning the turbulence model, which could also improve the duct flow agreement.

The computed and measured drag-coefficient trends with Reynolds number at M = 0.835, α = 2 deg are shown in Fig. 18. The computed dra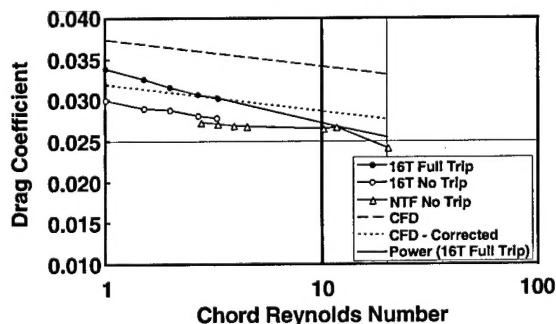g coefficients show an expected decrease in drag coefficient with an increase in Reynolds number. However, the fully turbulent computational results do not follow the same power law (slope of the log-log curve) as the 16T fully tripped data, nor do they follow the NTF data. The 16T results show a much larger decrease in drag than the computations. Since most of the change in drag coefficient is due to changing skin friction, the slope differences indicate that the computations do not accurately predict the change in skin friction with Reynolds number in 16T.

Wing and canopy comparisons between the computed and measured pressure coefficient are shown in Fig. 19 for α = 4 deg. For this case, the computations show massive separation at approximately mid-span of the wing while the data indicate only mild separation. The computations are clearly predicting an earlier onset of buffet. The onset of buffet occurs at slightly higher than four degrees (based on the criteria that the difference between the actual lift coefficient and the lift coefficient determined from a linear extrapolation of lift slope is 0.1). At present, CFD is not able to accurately predict separation and buffet onset or the variation of these phenomena with Reynolds number. Additional turbulence model development must be done to elevate CFD as a useful tool in the prediction of these phenomena.

Concluding Remarks

1. Since transonic wind tunnels used for production testing are not expected to achieve flight Reynolds number duplication in the foreseeable future, Reynolds number scaling will continue be required for future aircraft developments.

2. RNS has been used mainly to predict aircraft drag at flight RN. Heretofore, lift and moments have been observed to be relatively insensitive to Reynolds number and corrections have not normally been applied. However, there is a need to predict buffet boundary, which is sensitive to Reynolds number. Also, indications are that stability is sensitive to Reynolds number for tailless aircraft. Consequently, RNS procedures are needed to properly predict flight stability for these type configurations.

Fig. 18. Measured and computed trends with Re_c, M = 0.835, α = 2 deg, full trips.
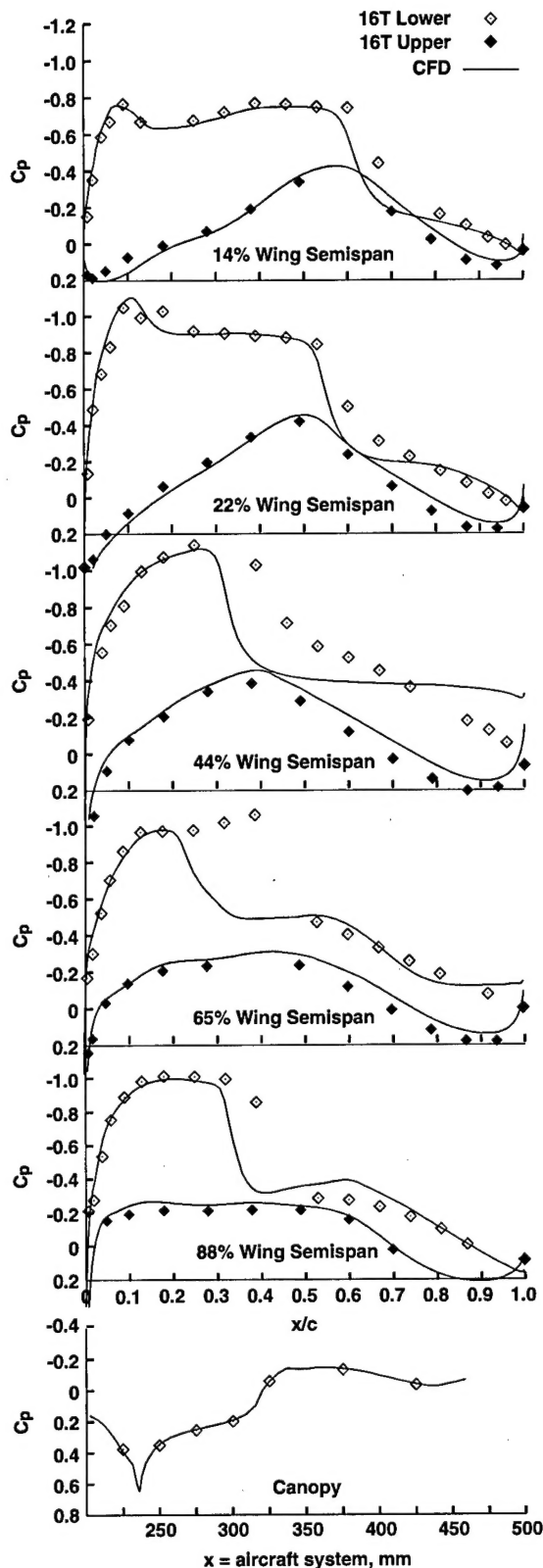
Fig. 19. Measured and computed model pressures, $M = 0.835$, $\alpha = 4$ deg, $Re_c = 2.7 \times 10^6$, full trips.

3. RNS alone is not sufficient to predict flight performance from low-Reynolds number wind tunnel data. Wind tunnel effects produce pseudo Reynolds number effects, which should be taken into account for best prediction of flight performance and comparing results between wind tunnels.

4. The computational results clearly show that the turbulence models (or perhaps just the calibration of the models) are deficient in predicting skin friction, as well as predicting onset of buffet in the wind tunnel. Additional effort must be directed towards tuning the turbulence models to provide the proper prediction of skin friction and momentum losses before CFD can be an accurate RNS tool. Since each tunnel has its own turbulence level, the tuned turbulence coefficients may be unique for each facility as well as for flight. In addition, this is only one case study and additional computations on other classes of configurations are needed. As mentioned, future military aircraft present additional challenges and are probably even more sensitive to Reynolds number scaling effects. Therefore, an additional database (similar to the TST database) on an advanced concept aircraft is needed. More validation testing has to be done.

5. Improvements in the prediction of flight aerodynamic performance of military aircraft are at least in part dependent on improvements in RNS and properly accounting for tunnels effects, including free-steam vorticity (turbulence) and spatial variations, wall and support interference, flow buoyancy, humidity, and various model effects, including aeroelasticity and fidelity.

References

1. Mack, M.D. and McMasters, John H. "High Reynolds Number Testing in Support of Transport Airplane Development," AIAA 17th Aerospace Ground Testing Conference, AIAA 92-3982, July 1992.

2. Flughum, D. A. "Navy Narrows F/A-18E/F 'Wing Drop' Options," *Aviation Week*, January 19, 1998.

3. Smith, J. E. "Transonic Wind Tunnels," *High Speed Problems of Aircraft and Experimental*

Methods, Volume VIII, Section F, Princeton University Press, 1961.

4. Haines, A.B. and Elsenaar, A. "An Outline of the Methodology." *Boundary Layer Simulation and Control in Wind Tunnels*, AGARD-AR-224, April 1988.

5. Haines, A. B. "Know Your Flow: The Key to Better Prediction and Successful Innovation," 36th Aerospace Sciences Meeting and Exhibit, AIAA 98-0221, January 1998.

6. Elsenaar, A. "Reynolds Number Effects and the Wind Tunnel Environment," *Boundary Layer Simulation and Control in Wind Tunnels*, AGARD AR 224, April 1988.

7. Sinclair, D.W. "Calculated Viscous Effects on Airfoils at Transonic Speeds." AIAA 88-2027, 1988.

8. Dougherty, N.S. Jr. "Influence of Wind Tunnel Noise on the Location of Boundary-Layer Transition on a Slender Cone at Mach Numbers from 0.2 to 5.5." AEDC-TR-78-44 (AD-A083166), March 1980.

9. Dougherty, N.S. Jr. and Fisher, D.F. "Boundary-Layer Transition Correlation on a Slender Cone in Wind Tunnels and Flight for Indications of Flow Quality." AEDC-TR-81-26 (AD-A111328), February 1982.

10. Fisher, D.F. and Dougherty, N.S. Jr. "In-Flight Transition Measurement on a 10-deg Cone at Mach Numbers from 0.5 to 2.0." NASA Technical Paper 1971, June 1982.

11. Sinclair, D.W. "A Comparison of Transition Reynolds Number Measured in a Wind Tunnel and In Flight." FED- Vol. 114, ASME/JSME Fluids Engineering Conference, Portland, OR, June 1991.

12. Benek, J. A., Steger, J. L., Dougherty, F. C., and Buning, P. G. "Chimera: A Grid-Embedding Technique." AEDC-TR-85-64 (AD-A-167466), April 1989.

13. Dietz, W. E. and Suhs, N. E. "PEGSUS 3.0 User's Manual." AEDC-TR-89-7 (AD-A211974), April 1986.

14. Tramel, R.W., and Nichols, R. H. "A Highly Efficient Numerical Method For Overset-Mesh Moving-Body Problems." AIAA Paper No. 97-2040, June, 1997.

15. Nichols, R. H. "A Two-Equation Model for Compressible Flows." AIAA Paper No. 90-0494, January, 1990.

16. Speziale, C. G., Ridha, A. and Anderson, E. C. "A Critical Evaluation of Two-Equation Models for Near-Wall Turbulence." ICASE Report No. 90-46, June 1990.

17. Nichols, R. H. "Development and Validation of a Two-Equation Turbulence Model with Wall Functions for Compressible Flows." AIAA 96-2385, June 1996.

18. White, F. M. and Christoph, G. H. "A Simple Analysis of Compressible Turbulent Two-Dimensional Skin Friction Under Arbitrary Conditions." AFFDL-TR-70-133, Wright-Patterson AFB, OH, February 1971.

19. Chan, W. M. "User's Manual for FOMOCO Utilities – Force and Moment Computation Tool for Overset Grids." NASA TM 110408, July 1996.

20. Sellers, M. E. "Pressure Sensitive Paint Data on the Transonic Technology Wing Demonstrator (TST) in the AEDC Propulsion Wind Tunnel 16T." AEDC-TR-98-3, to be published.

21. Buning, P. G., et al. *Overflow User's Manual*, Version 1.8, NASA Langley Research Center, Hampton, VA, February 1998.